Int J CARS (2015) 10:707–715
DOI 10.1007/s11548-015-1209-y

ORIGINAL ARTICLE

Computer-assisted hip resurfacing planning using Lie group shape models

Mohamed S. Hefny[1] · **John F. Rudan**[2] · **Randy E. Ellis**[1]

Received: 18 February 2015 / Accepted: 3 April 2015 / Published online: 1 May 2015

Abstract
Introduction Hip resurfacing is a surgical option for osteoarthritis young and active patients. Early failures has been reported due to improper implant placement. Computer-assisted surgery is a promising avenue for more successful procedures.
Purpose This paper presents a novel automatic surgical planning for computer-assisted hip resurfacing procedures. The plan defined the femoral head axis that was used to place the implant. The automatic planning was based on a Lie group statistical shape model.
Methods A statistical shape model was constructed using 50 femurs from osteoarthritis patients who underwent computer-assisted hip resurfacing. The model was constructed using product Lie groups representation of shapes and nonlinear analysis on the manifold of shapes. A surgical plan was drawn for the derived base shape. The base shape was transformed to 14 femurs with known manual plans. The transformed base plan was used as the computed plan for each femur. Both actual and computed plans were compared.
Results The method showed a success by computing plans that differ from the actual plans within the surgical admissible ranges. The minimum crossing distance between the two plans had a mean of 0.75 mm with a standard deviation of 0.54 mm. The angular difference between the two plans had the mean of 5.94° with a standard deviation of 2.14°.
Conclusion Product Lie groups shape models were proved to be successful in automatic planning for hip resurfacing computer-assisted surgeries. The method can be extended to other orthopedic and general surgeries.

Keywords Surgical planning · Orthopedics · Computer-aided decision · Lie groups

Introduction

Hip resurfacing is a surgical treatment for osteoarthritis that is gaining popularity over total hip replacement, mainly for young and active patients [2,3,31]. Hip resurfacing procedures preserve bone stock loss by less bone removal. The preservation of original bone allows easier revisions. Also, the implant has less chance of dislocation due to the larger head size and has better wear properties.

Hip resurfacing is recognized as a technically challenging procedure with difficult surgical exposures [2,4,31,40]. Improper implant placement can produce postoperative complications such as: notching of the femoral neck, with an increased risk of postoperative fracture; incomplete reaming of the head, resulting in poor bonding of prosthetic to bone; an unstable joint, with an increased risk of postoperative dislocation; and edge loading of the prostheses, which may increase the production of metal particles through wear.

Conventional planning and computer-assisted planning of the femoral component aim to maintain the patient's anatomical stem–shaft angle (which is the angle of the component stem to the femoral shaft) and simultaneously to avoid notching the femoral neck. Conventional technique, recommended by most implant manufacturers, is to preoperatively plan

✉ Mohamed S. Hefny
hefny@cs.queensu.ca

John F. Rudan
rudanj@kgh.kari.net

Randy E. Ellis
ellis@cs.queensu.ca

[1] School of Computing, Queen's University, Kingston, ON K7L 2N8, Canada

[2] Department of Surgery, Queen's University, Kingston, ON K7L 2V7, Canada

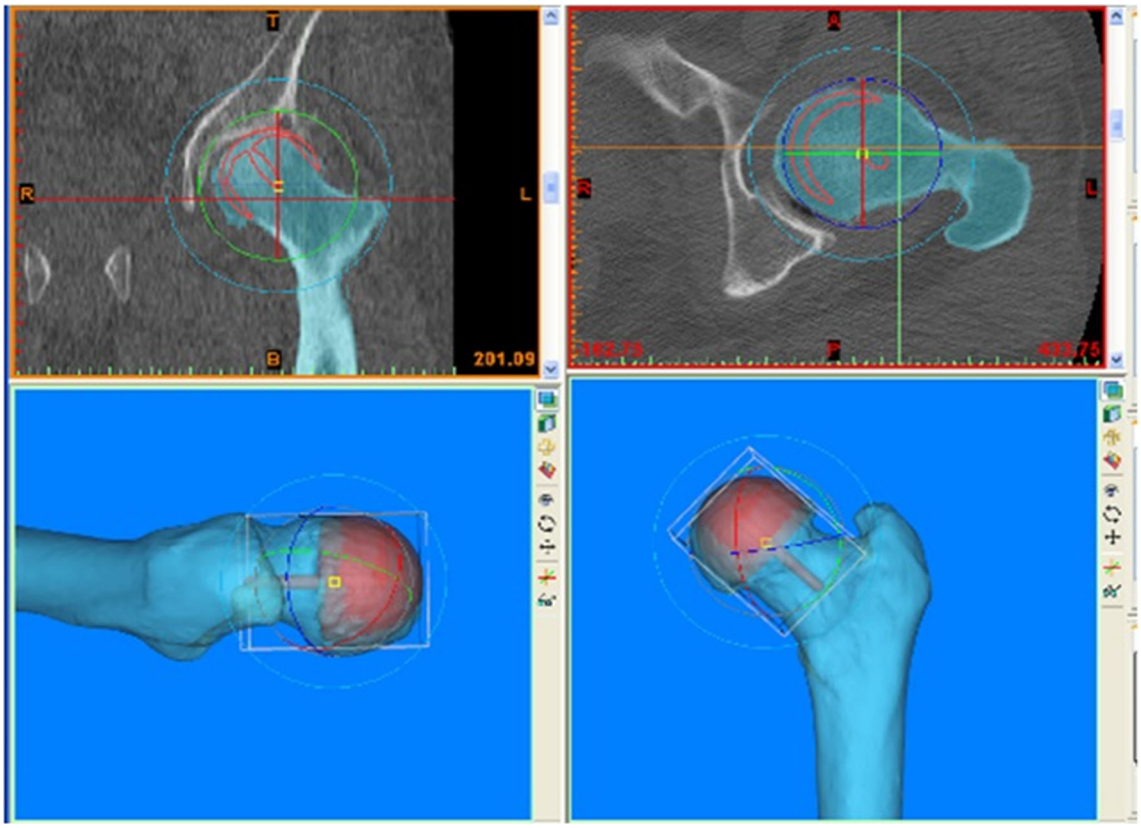

Fig. 1 Hip resurfacing plan using Mimics (Materialise, Leuven, BE)

from a standing anterior–posterior (AP) radiograph to estimate the implant size and angulation. Computer-assisted planning can replicate this process but, preferably, uses a 3D preoperative model to provide a full spatial plan and ensure that the version angle of the implant also respects the highly variable anatomy of the femoral neck. Because these anatomical and biomechanical constraints are common to all implants, they are largely replicated in computer-assisted systems; in the Methods section, we describe the method of Kunz et al. [30] as an example, but very similar methods are used in other systems that have been reported.

Computer-assisted orthopedic surgery methods have been used to enhance the procedure and to reduce the risk of implant failure. Figure 1 shows a hip resurfacing surgical plan drawn in our institution using Mimics (Materialise, Leuven, BE). Hess et al. [27] reported the first use of 2D fluoroscopy to navigate the femoral head for hip resurfacing. Belei et al. [8] presented an alternative method for 2D fluoroscopy. With the increase in 3D imaging technologies, Hodgson et al. [28] presented using computed tomography (CT) for resurfacing navigation. Davis et al. [12] adapted image-free navigation approach. All those systems used optoelectronic technologies for intra-operative tracking of anatomy and instruments. Barrett et al. [7] described intra-operative mechanical tracking system and reported improved results over other tracking technologies. Kunz et al. [30] presented the use of individualized drill guides using a 3D printing technology.

A specific aspect of computer-assisted hip resurfacing is the question of how accurate a plan must be for it to produce good surgical outcomes. Our review of the literature suggests that a stem–shaft angular difference of 10° is clinically acceptable. Olsen et al. [33] deemed all of the 100 patients in their series to have clinically acceptable results, with stem–shaft angles limited to at most 8° of difference. Zhang et al. [42] studied 20 patients with clinically acceptable results, having stem–shaft deviations of $10° \pm 1.5°$. Most recently, Du et al. [13] found, for 16 patients, stem–shaft deviations of at most 9°.

These clinical data imply that if the error of the plan plus implantation error is less than about 10°, then the outcomes are most likely to be acceptable. For all of the studies cited, the implantation errors—both in vitro and in vivo—are at most 2°. Consequently, for the purposes of this study, a limit of 8° of angular deviation was taken to be the goal of automated planning.

This paper proposes the use of Lie groups statistical shape models to automatically plan a hip resurfacing procedure with computer assistance. The method uses a class of matrix manifolds, namely Lie groups, to construct a statistical shape

model of the anatomy. Lie groups are powerful mathematical structures that are algebraic groups and smooth manifolds at the same time. Being algebraic groups enables performing efficient inexpensive computations, and being smooth manifolds enables performing accurate nonlinear statistics on the shape space. The derived base shape from the model is planned for surgery and transformed to the patient anatomical image. The transformed plan is used as the automatically computed plan. The computed method is compared to actual planned surgeries for validation and verification.

This work has two main contributions. First, it presents a new method of statistical shape model construction using Lie groups. The method differs from our previous work [23,25,26] that it is directly applied to triangular meshes produced by most commercial applications and does not require transforming the surfaces to quadrilateral meshes. Second, this is the first report on using statistical shape models to hip resurfacing surgical planning. All previous work required a patient-specific plan.

The rest of this paper has a straightforward structure. "Background" covers the required technical background for both statistical shape models and matrix manifolds. The methods are detailed in "Methods." Results comparing the computed plans using the method and actual plans are presented and discussed in "Experiments and results." "Conclusion" draws the conclusions of this study.

Background

This section covers the essential background to develop the methods presented in this paper. It defines statistical shape models and highlights the key developments in the literature including both linear and nonlinear methods. It also summarizes the related concepts from matrix manifolds, mainly Lie groups.

Statistical shape models

A statistical shape model is a mathematical structure representing the shape variability. Such a model uses measures of statistics that come from geometrical descriptions of samples of a population. A highly influential development was the point distribution model [10,11], which has been widely used in many general applications. A point distribution model relies on principal component analysis [29,34] and assumes that shapes can be described in a Euclidean space. Shapes that are better described in a nonlinear space confound such analytical methods.

An object is represented by a set of landmarks that have an established point correspondence over a population. Landmarks can be anatomical features identified by an expert, or might be geometrical features associated with a mathematical shape. In shape analysis, landmarks usually provide a relatively dense representation of shape. For example, a computer representation of a 2D contour is a set of connected points.

In this representation, training data typically consisted of k objects. Each object is represented using m points $p \in \mathbb{R}^n$, where n is either 2 or 3. Because each object is naturally in a $\mathbb{R}^{n\times m}$ space, it is represented as a vector of high dimension. For the $3D$ case, an object S is commonly represented as

$$S = \left({}^{x}_{1}p,\ {}^{y}_{1}p,\ {}^{z}_{1}p, \ldots,\ {}^{x}_{m}p,\ {}^{y}_{m}p,\ {}^{z}_{m}p\right)$$

Distinct objects have distinct representation vectors, with natural correspondences between the points from which each representation vector is produced. Linear statistics can be easily applied to those vector structures, and shapes can be easily reproduced.

Nonlinear statistical shape analysis has been studied by only few research groups. Fletcher et al. [16–18] presented principal geodesic analysis (PGA). The method was initially applied to medial representations and later to diffusion tensor imaging [14,15]. PGA was a generalization of PCA from vector spaces to manifolds. PGA provided a general framework for using exponential mapping to linearize manifolds.

PGA was an approximation of the data samples on the tangent space that assumed localization of the data around an intrinsic mean. Sommer et al. [41] introduced exact-PGA that performed intrinsic computations on the manifold instead of using the simplifying mapping to the tangent space. The work concluded that PGA performed well on some data but did not provide acceptable approximations for other data sets. It was also observed that the exact-PGA computation was very expensive, compared to the cost of PGA that used the tangent vector space.

PGA was, overall, more efficient than exact-PGA but less accurate when applied to some data sets. The application to diffusion tensors required manipulating the data to fit the criteria of symmetric positive-definite matrices, an alternative that is not always possible for other empirical data.

Pennec et al. [35–37] used a *random primitive* as an equivalent to a random variable on the manifold. Based on this idea, the main statistical tools were defined. In related work, Arsigny et al. [5,6] provided Log-Euclidean metrics as tools to perform fast computations of smooth manifold spaces using the exponential mapping to vector spaces. This was based on finding a one-to-one mapping between symmetric matrices and vector spaces that enabled the use of vector addition and scalar multiplication via exponential maps. The Log-Euclidean framework was an easier and less expensive alternative to PGA that used matrices as Lie groups and the matrix exponential as a linearization tool. The Log-Euclidean framework was first developed for symmetric matrices and applied to diffusion tensor images, which was straightforward because those matrices are symmetric and positive-definite.

Freifeld et al. [20] developed the Lie bodies concept, which modeled body shapes using principal geodesic analysis on Lie group structures. They modeled shapes as a collection of triangular meshes. A Lie group structure is constructed by the product of 3D rotation in space and shape deformation on 2D plane. The method dropped the translation factor from the computation and analysis, and used a least-squares fitting algorithm to construct the shapes after analysis. The method was applied to analyze body scans of adult women and has not been reported for any further use.

Hefny et al. [23] identified the Lie group of homogeneous matrices as a matrix Lie group and used this group to analyze shapes. The method was used to analyze 2D femoral head–neck contours [24], 3D femoral heads [26] and 3D distal radii [25]. The 3D version of the method required quadrilateral meshes, which is suitable for tomographic imaging that deals with shapes as slices and allows the easy construction of meshes using a stack of 2D contours. The method was not applicable to triangular meshes that are the legacy of 3D shape meshes.

Matrix manifolds

The concept of the matrix manifold is at least one century old [38] but has seen increasing recent use in mathematics and physics. This concept is the foundation for many applications in mathematical physics, from elementary particles to cosmological principles [39]. Only in the last decade have matrix Lie groups, a special case of matrix manifolds, started to attract the attention of computer scientists, primarily in computer vision and image analysis. The use of a matrix manifold, in particular, makes it possible to use differential-geometry tools to analyze nonlinear spaces.

A Lie group $\mathbb{G}_{\mathbb{L}}$ is formally defined as a group $\mathbb{G}$ and a smooth manifold $\mathcal{M}$ such that the group operation $g \circ h \rightarrow k$ is a smooth map $\mathbb{G}_{\mathbb{L}} \circ \mathbb{G}_{\mathbb{L}} \rightarrow \mathbb{G}_{\mathbb{L}}$, and the inverse $g \rightarrow g^{-1}$ is a smooth map $\mathbb{G}_{\mathbb{L}} \rightarrow \mathbb{G}_{\mathbb{L}}$ [22]. The unification of group and manifold properties into a Lie group arises from the smoothness requirement imposed on both the group operation and the inverse property [21].

Each Lie group has an associated Lie algebra. A Lie algebra can be constructed by linearizing a Lie group. The linearization is typically done by expanding the group combinatorial operator about the coordinates of the group elements at any given group element. The linearization of the Lie group forms a new set of elements that are the Lie algebra. A Lie algebra is a linear vector space, which permits linear operations and statistics to be computed on the Lie algebra.

An exponential map is a method for transforming between a manifold and a tangent space or, equivalently, between a Lie group and a Lie algebra. For matrix Lie groups, this transformation is simply the matrix exponential (to map a tangent vector to a matrix) or the matrix logarithm from which non-trivial entries are extracted to form a tangent vector. Analytically, for every $n \times n$ real matrix M, the exponential e^M is a continuous function of M that uniformly converges; it can be defined as a Taylor series

$$e^M = \sum_{k=0}^{\infty} \frac{M^k}{k!}$$

The matrix exponential has a straightforward computation. An elementary observation in linear algebra is that any square matrix is either diagonalizable, nilpotent, or decomposable to both [22]. Here, we represent an affine transformation $\hat{M}$ as a homogeneous matrix; any such matrix can be expressed as the product of a dilation or scaling matrix, pre-multiplied by a shear matrix, pre-multiplied by a rotation matrix and pre-multiplied by a translation matrix. This decomposition is

$$\hat{M} = \hat{L}\hat{R}\hat{H}\hat{E}\hat{G}$$

The matrix logarithms of a translation matrix $\hat{L}$ and a shear matrix $\hat{H}$ is both nilpotent of degree 2; the logarithm of a scaling matrix $\hat{G}$ is diagonal, and the logarithm of an orthogonal rotation matrix $\hat{R}$ is a skew-symmetric matrix. Any non-singular homogeneous matrix $\hat{M}$ can easily be decomposed into products, from which the logarithms can be found, from which the independent components can be extracted and assembled into a tangent vector.

From this brief mathematical background, it can be supposed that a shape might be represented as a matrix Lie group using one or more representations. Such a representation would provide a mapping of data between a nonlinear manifold and the associated linear tangent space, thus enabling simple computations to be performed on complicated structures. The principal advantage of using a matrix Lie group is that one does not have to perform numerical estimations on the manifold, which must be done for PGA and exact-PGA: the transformation of one manifold point to another is equivalent to transformation of one group element to another, which is a closed-form computation in any Lie group and is simply matrix multiplication in a matrix Lie group.

Methods

This section develops the methods that are the main contribution of this paper. It describes the construction of a shape model using a product Lie group, which is derived from triangular meshes of anatomical shapes extracted from medical images. Using a product Lie group enables performing efficient and accurate computations in the nonlinear space of shapes, while standard point cloud methods assumes linearity of the space. It also describes the use of the model to automatically compute the plan.

Model construction

A new product Lie group representation of shape is developed. This representation enables analyzing triangular meshes with no extra processing either before or after the analysis.

For model construction, a data set consists of a population of shape samples consisting of triangular meshes with some number of corresponding triangles. Each sample can be handled as an ensemble of triangles. This method constructs product Lie group elements to represent the transformation between each triangle in the base shape to the corresponding triangle in each sample shape.

A simple scenario is shown in Fig. 2. Any triangle $\triangle A$ in 3D Cartesian space can be mapped to another triangle $\triangle B$ by a 3D rigid transformation T consisting of rotation and translation and a 2D deformation D consisting of shear and scale. First, the triangle $\triangle A$ can be transformed to the 2D Cartesian xy-plane using rotation and translation. This is a shape-preserving transformation, and the transformed triangle is called canonical triangle. Second, the canonical triangle $\triangle A$ shape can be deformed to the shape of canonical triangle $\triangle B$ using 2D shear and scaling. Finally, the deformed triangle $\triangle A$ can be transformed to the original triangle $\triangle B$ using rigid 3D transformation. This sequence forms 3D affine transformations in 3D space with a specific structure that allows efficient and effective analysis with simple implementation.

A base shape in a 3D Cartesian space is identified. The word base is carefully used instead of mean because in the manifold space, a mean may not be unique or may not even exist. The base shape is the shape that is most likely in equivalent distance to all samples in the data set. On a manifold, the mean can be approximated using Frèchet's algorithm [19].

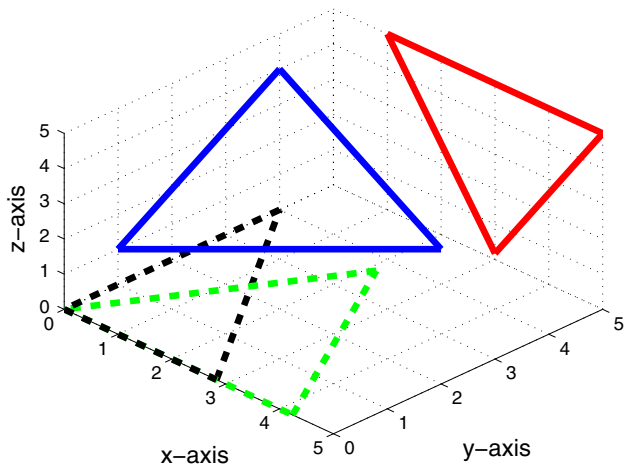

Fig. 2 Triangle $\triangle A$ (*blue*) is transformed to the canonical form (*green*), deformed to the canonical form of triangle $\triangle B$ (*black*), and transformed to the original triangle $\triangle B$ (*red*)

We use the term "altered" to describe a shape other than the base shape.

Each triangle forms a coordinate frame, in general not rectilinear, consisting of an origin vertex and two vectors in the 3D Cartesian space. Each coordinate frame could be represented by a homogeneous matrix. The triangle can also be transformed to a canonical triangle in 2D Cartesian space by a translation and a rotation, that is, by a rigid homogeneous transformation.

A non-degenerate triangle $\triangle P$ can be represented as

$$P = \begin{bmatrix} p_i^x & p_j^x & p_k^x \\ p_i^y & p_j^y & p_k^y \\ p_i^z & p_j^z & p_k^z \\ 1 & 1 & 1 \end{bmatrix} \tag{1}$$

where the order of the points p_i, p_j, and p_k is arbitrary selected. Geometrically, the triangle $\triangle P$ can be transformed in 3D Euclidean space by the homogeneous rigid transformation

$$\hat{T} = \begin{bmatrix} R & \mathbf{d} \\ \mathbf{0}^T & 1 \end{bmatrix}$$

where $R \in \mathbb{SO}(3)$ is a 3D rotation matrix and $\mathbf{d} \in \mathbb{R}^3$ a 3D translation vector. The matrix $\hat{T}$ is in the homogeneous transform Lie group $\mathbb{H}(4)$ [23]. Equivalently, a matrix transformation $\hat{T}$ of the triangle $\triangle P$ is a point in the manifold $\mathcal{H}(4)$ of homogeneous transform matrices of degree 6. The matrix $\hat{T} \in \mathbb{H}(4)$ is an operator that drags one point to another on the manifold. One interesting transformation takes a triangle to a canonical form by translating one vertex to the origin and rotating the triangle to align one of the edges with the x-axis. For such a transformation, $\hat{T}$, p_i is restricted to the origin $[0\,0\,0]^T$, so the canonical triangle $\triangle P$ is represented by the matrix

$$\hat{D} = \begin{bmatrix} p_j^x & p_k^x \\ 0 & p_k^y \end{bmatrix}$$

The matrix $\hat{D}$ of a canonical triangle represents its shape. A canonical triangle can be scaled by independently varying p_j^x or p_k^y or sheared by varying p_k^x and p_k^y. The matrix $\hat{D}$ belongs to the group $\mathbb{B}(2)$ which is the Lie group of square upper triangular matrices of degree 2.

The transformation Lie group $\mathbb{H}(4)$ and the deformation Lie group $\mathbb{B}(2)$ can be combined by the product Lie group

$$\mathbb{M}(6) = \mathbb{H}(4) \times \mathbb{B}(2)$$

A particularly convenient representation of the Cartesian product of two matrix Lie groups is to create a larger matrix with a block-diagonal structure. For spatial triangles, the elements of the $\mathbb{M}(6)$ group will have the form

$$M = \begin{bmatrix} \hat{T} & 0 \\ 0 & \hat{D} \end{bmatrix} \tag{2}$$

The transformation and deformation matrices do not interact through the new group operation, which implies that the properties of the original manifolds are preserved. This can readily be seen by the simple matrix computation

$$\begin{bmatrix} \hat{T}_2 & 0 \\ 0 & \hat{D}_2 \end{bmatrix} \begin{bmatrix} \hat{T}_1 & 0 \\ 0 & \hat{D}_1 \end{bmatrix} = \begin{bmatrix} \hat{T}_2\hat{T}_1 & 0 \\ 0 & \hat{D}_2\hat{D}_1 \end{bmatrix}$$

The great utility of the representation in Eq. 2 is that it decouples the rigid transformation of a triangle in 3D space from its canonical shape. This has 9° of freedom, which is a lower dimensional representation than using a 3D affine transformation that has 12° of freedom.

In preparation for analysis, any altered triangle $\triangle A$ can be mapped to a base triangle $\triangle B$ through a transformation C as $A = CB$. The transformation C is equivalent to

$$C = \hat{T}_B^{-1}\hat{D}_A\hat{T}_A$$

where T_A is transformation of the altered triangle $\triangle A$ to its canonical form, D_A is the deformation of $\triangle A$ in its canonical form to the canonical form of the base triangle $\triangle B$, and T_B is the transformation of $\triangle B$ to its canonical form.

For each matrix C, there is a unique logarithmic mapping to a matrix K such that $e^{(K)} = C$. For each such matrix K, there is an associated vector $\mathbf{k}$. All such vectors $\mathbf{k}$ that transform an altered shape A to the base shape B can be assembled in a vector $\mathbf{m}$, and all such vectors for a set of shapes can be assembled into a matrix M. The singular-value decomposition of each matrix is the familiar $M = U\Sigma V^T$.

The matrix exponential maps the transformations from the nonlinear manifold space to the linear space of its tangent. Mathematically, this enables using the singular-value decomposition which is one form of principal component analysis.

Plan computation

The planning of the operative cases used in this study followed the methodology described by Kunz et al. [30]. In hip resurfacing computer-assisted surgery, a plan is manually drawn by a surgeon using the navigation software system. This plan defines, among other parameters, the femoral head–neck axis. This axis is used to guide the drilling and prosthesis alignment. The automatic computation of the plan presented here was done using the shape model constructed in the previous subsection.

Briefly, the preoperative plan could be performed using custom software or recent versions of commercial software. The proximal femur was segmented in the preoperative CT scan by a single technician who prepared most of the operative cases for the research team. A 3D computational model of a proposed femoral component was brought into the segmentation and visually aligned to the femoral head by the surgeon who performed the surgery (author JFR). The component's stem axis was visually aligned to the femoral neck axis and positioned to completely cover the cartilage that was damaged by osteoarthritis. This alignment process included selection of the component size and component position, because along with the stem angle, these geometric parameters interacted in providing adequate bone coverage without notching or excessive gap filling with bone cement.

The base shape of the statistical shape model was then transformed to the patient femur. The plan of the base shape was also transformed to the patient anatomy along with the surface shape. This transformed plan defined the computed plan of the patient. This method required the manual plan to be done once for the base shape and could subsequently be used for any number of patients. Only a simple automatic registration was required to compute the patient-specific plan.

Experiments and results

This section describes the experiments conducted to validate and verify the methods presented in the previous section. It presents the data collection and preparation processes. Then, it evaluates the methods when applied to the prepared data.

Data collection and preparation

CT scans were obtained from patients who underwent computer-assisted hip resurfacing surgeries in our affiliated hospital. All patients consented using their medical images in research. The data collection was approved by the relevant institutional review board (IRB). The images were acquired using a GE Lightspeed 16-slice CT scanner (General Electric, Milwaukee, USA) with a moving gantry; axial images had a 1.25-mm slice thickness reconstructed from automatic tube current modulation.

The femurs of the patients were segmented, and corresponding meshes were constructed in the CT scans as part of the procedure. All CT image processing were performed using Mimics (Materialise, Leuven, BE). The data meshes were post-processed for gap filling using MeshLab [1]. All meshes were reduced to have 2000 triangles and 1002 points. The meshes were aligned to an arbitrarily selected base mesh using the iterative closest point registration algorithm [9]. A non-rigid registration was performed, to establish the point correspondences between meshes, using coherent point drift [32]. Both registration methods were implemented using MATLAB (Mathworks, Natick, USA).

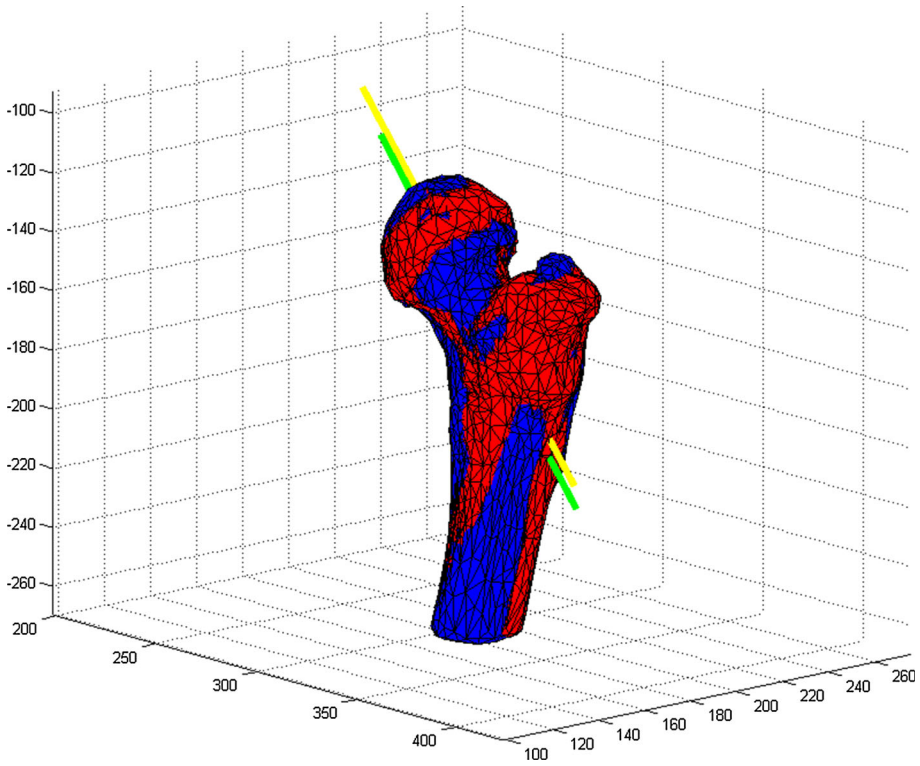

Fig. 3 Actual plan (*yellow*) and computed plan (*green*) are drawn against the triangular meshes of a patient femur (*red*) and fitted mesh (*blue*)

A data set of 50 femurs was used to construct the shape model. One shape was selected to be deformed to other shapes for establishing points correspondence. This base shape was removed from the data set to eliminate any bias of dominating features of this shape.

Validation and verification

To verify the automatic planning, a data set of 14 femurs was selected from the overall 50 samples. The drilling plans were created by an orthopedic surgeon for actual performed surgery. In order to verify our method, we chose to compare our results with successful plans created by a senior surgeon; a successful plan was one that did not require a surgical revision. Here, we refer to the successful plan created by the surgeon as the actual plan. The base shape was transformed to each data sample. The plan of the base shape was transformed along with shape. The transformed base plan was defined as the computed plan. The computed plan was compared to the actual plan in terms of the minimum crossing distances and the angular differences between the two axes. A representative automatic plan and the actual plan are shown in Fig. 3. The results are reported in Table 1.

Most of the automatic plans showed a minimum crossing distance with less than one millimeter which is negligible in orthopedic procedures. With the exception of two outliers, all distances were less than 2 mm. The mean without the outliers was 0.75 mm with a standard deviation of 0.54 mm.

Table 1 Minimum crossing distances and angular differences

Sample	Minimum crossing distances (mm)	Angular differences (degrees)
1	0.98	11.28
2	0.11	9.72
3	0.85	7.54
4	0.45	7.73
5	0.47	5.89
6	0.44	8.54
7	0.67	3.24
8	5.45	6.85
9	4.40	2.68
10	1.97	6.83
11	0.75	4.24
12	1.53	5.43
13	0.11	4.39
14	0.70	4.18

This results show that the difference between the lines is less than the diameter of the drill bit.

Also, most of the samples showed angular differences between the automatic plan and the actual plan $<10°$ with the exception of one sample. The mean angular difference without the outlier was 5.94° with a standard deviation of 2.14°. The computed angular differences are within the acceptable ranges for such surgeries, as identified from the existing literature in the Introduction.

The results show that the computed plans are the acceptable plans for hip resurfacing computer-assisted surgeries. This provides a reliable recommendation for the surgeon and enhances the outcomes. One benefit of the automatic planning is using an accurate plan created by a senior surgeon to assist less senior ones. In sum, the novel automatic method is valid for immediate clinical trials.

Conclusion

Hip resurfacing is the procedure of choice for young and active osteoarthritis patients due to its better outcomes. Poor surgical planning is implicated in early prosthesis failures. This work aims to enhance the planning process by using shape models constructed using Lie groups.

Medical images of femurs were obtained from patients who underwent computer-assisted hip resurfacing surgery. Each femur had an associated actual plan drawn by the performing surgeon. A statistical shape model was constructed using 50 femurs. A base shape was derived from the data set. The base shape was transformed to each of 14 patient femurs. The plan associated with the base shape was transformed with the same registration. The transformed plan was identified as the computed plan for each patient femur. The actual plans are compared to the computed plans.

The variation between the computed plans and the actual plans was within the surgical acceptable limits. A mean of 0.75 mm with a standard deviation of 0.54 mm of infinite minimum distance and a mean of 5.94° with a standard deviation of 2.14° of the angular difference were calculated between the two axes. In this study, the method was compared to plans created by one surgeon. Inter-surgeon variability is a subject for future work.

In sum, this paper presents a first report on using Lie groups shape models for automatic planning of computer-assisted hip resurfacing surgery. The method can enhance computer-assisted hip resurfacing planning by automating accurate planning that reduces revisions by creating a clinically acceptable drilling path. The drilling path determines the location of the implant with respect to the anatomy. A tilted implant may cause complications that require revisions. Immediate extensions to other orthopedic and general surgeries, such as image-guided percutaneous scaphoid fixation and prostate cancer brachytherapy, are possible and promising.

Acknowledgments This work was supported in part by the Canada Foundation for Innovation, the Canadian Institutes of Health Research, Kingston General Hospital, the Ontario Research and Development Challenge Fund, and the Natural Sciences and Engineering Research Council of Canada.

Conflict of interest Mohamed S. Hefny, John F. Rudan, and Randy E. Ellis declare that they have no conflict of interest.

Ethical standard The relevant institutional review board (IRB) approved the data collection process. Informed consent was obtained from all patients for being included in the study.

References

1. Meshlab. http://meshlab.sourceforge.net/
2. Amstutz HC (2006) Hip resurfacing arthroplasty. J Am Acad Orthop Surg 14:452
3. Amstutz HC, Ball ST, Le Duff MJ, Dorey FJ (2007) Resurfacing tha for patients younger than 50 year: results of 2- to 9-year followup. Clin Orthop Relat Res 460:159
4. Amstutz HC, Campbell PA, Le Duff MJ (2004) Fracture of the neck of the femur after surface arthroplasty of the hip. J Bone Joint Surg Am 86–A:1874
5. Arsigny V, Pennec X, Ayache N (2005) Polyrigid and polyaffine transformations: a novel geometrical tool to deal with non-rigid deformations—application to the registration of histological slices. Med Image Anal 9(6):507–523
6. Arsigny V, Pennec X, Ayache N (2006) Log-Euclidean metrics for fast and simple calculus on diffusion tensors. Magn Reson Med 56(2):411–421
7. Barrett AR, Davies BL, Gomes MP, Harris SJ, Henckel J, Jakopec M, Kannan V, Rodriguez Y, Baena FM, Cobb JP (2007) Computer-assisted hip resurfacing surgery using the acrobot navigation system. Proc Inst Mech Eng H 221:773
8. Belei P, Skwara A, De La Fuente M, Schkommodau E, Fuchs S, Wirtz DC, Kämper C, Radermacher K (2007) Fluoroscopic navigation system for hip surface replacement. Comput Aided Surg 12:160
9. Besl PJ, McKay ND (1992) A method for registration of 3-D shapes. IEEE Trans Pattern Anal Mach Intell 14(2):239–256
10. Cootes TF, Taylor CJ, Cooper DH, Graham J (1992) Training models of shape from sets of examples. In: Proc. British Machine Vision Conference. Springer, London, pp 9–18
11. Cootes TF, Taylor CJ, Cooper DH, Graham J (1995) Active shape models-their training and application. Comput Vis Image Underst 61(1):38–59
12. Davis ET, Gallie P, Macgroarty K, Waddell JP, Schemitsch E (2007) The accuracy of image-free computer navigation in the placement of the femoral component of the birmingham hip resurfacing: a cadaver study. J Bone Joint Surg Br 89:557
13. Du H, Tian XX, Li TS, Yang JS, Li KH, Pei GX, Xie L (2013) Use of patient-specific templates in hip resurfacing arthroplasty: experience from sixteen cases. Int Orthop 37(5):777–782
14. Fletcher PT, Joshi S (2004) Principal geodesic analysis on symmetric spaces: Statistics of diffusion tensors. In: ECCV Workshops CVAMIA and MMBIA, 3117. pp 87–98
15. Fletcher PT, Joshi S (2007) Riemannian geometry for the statistical analysis of diffusion tensor data. Signal Proc 87:250–262
16. Fletcher PT, Joshi S, Lu C, Pizer SM (2003) Gaussian distributions on Lie groups and their application to statistical shape analysis. Inf Process Med Imaging 18:450–462
17. Fletcher PT, Lu C, Joshi S (2003) Statistics of shape via principal geodesic analysis on Lie groups. IEEE Comput Soc Conf Comput Vis Pattern Recogn 1:95–101
18. Fletcher PT, Lu C, Pizer SM, Joshi S (2004) Principal geodesic analysis for the study of nonlinear statistics of shape. IEEE Trans Med Imaging 23(8):995–1005
19. Fréchet M (1948) Les éléments aléatoires de nature quelconque dans un espace distancié. Ann Inst H Poincaré 10:215–310

20. Freifeld O, Black MJ (2012) Lie bodies: a manifold representation of 3D human shape. Eur Conf Comput Vis LNCS 7572:1–14
21. Gilmore R (2008) Lie groups, physics, and geometry. Cambridge University Press, Cambridge
22. Hall BC (2003) Lie groups, Lie algebras, and representations. Springer, Berlin
23. Hefny MS (2014) Analysis of discrete shapes using lie groups. Ph.D. thesis, Queen's University
24. Hefny MS, Ellis RE (2013) A statistical shape model of femoral head-neck cross sections using principal tangent components. Proceedings on IEEE International Symposium Biomedical Imaging, pp 89–92
25. Hefny MS, Pichora DR, Rudan JF, Ellis RE (2014) Manifold statistical shape analysis of the distal radius. Int J Comp Assist Surg 9(SUPP 1):S35–S42
26. Hefny MS, Rudan JF, Ellis RE (2014) A matrix lie group approach to statistical shape analysis of bones. Stud Health Technol Inform 196:163–169
27. Hess T, Gampe T, Koettgen C, Hess T (2004) Intraoperative navigation for hip resurfacing. methods and first results. Orthopade 33:1183
28. Hodgson AJ, Inkpen KB, Shekhman M, Anglin C, Tonetti J, Masri BA, Duncan CP, Garbuz DS, Greidanus NV (2005) Computer assisted femoral head resurfacing. Comput Aided Surg 10:337
29. Hotelling H (1933) Analysis of a complex of statistical variables into principal components. J Educ Psychol 24:417–441
30. Kunz M, Xenoyannis GL, Rudan JF, Ellis RE (2010) Computer-assisted hip resurfacing using individualized drill templates. J Arthroplasty 25(4):600–606
31. Mont MA, Ragland PS, Etienne G, Seyler TM, Schmalzried TP (2006) Hip resurfacing arthroplasty. J Am Acad Orthop Surg 14:454
32. Myronenko A, Song X (2010) Point-set registration: coherent point drift. IEEE Trans Pattern Anal Mach Intell 32(12):2262–2275
33. Olsen M, Naudie DD, Edwards RW, Schemitsch EH (2009) Evaluation of a patient specific femoral alignment guide for hip resurfacing. J Arthroplasty 29:590–595
34. Pearson K (1901) On lines and planes of closest fit to system of points in space. Philos Mag 6(2):559–572
35. Pennec X (1999) Probabilities and statistics on Riemannian manifolds: a geometric approach. IEEE Workshop on Nonlinear Signal and Imag Proc, pp 1994–198
36. Pennec X (2006) Intrinsic statistics on Riemannian manifolds: basic tools for geometric measurements. J Math Imag Vis 25:127–154
37. Pennec X, Fillard P, Ayache N (2006) A Riemannian framework for tensor computing. Int J Comput Vis 66:41–66
38. Scholz E (1999) The concept of manifold, 1850–1950. In: James IM (ed) History of topology. Elsevier, Amterdam, pp 25–64
39. Schutz B (1980) Geometrical methods of mathematical physics. Cambridge University Press, Cambridge
40. Siebel T, Maubach S, Morlock MM (2006) Lessons learned from early clinical experience and results of 300 asr hip resurfacing implantations. Proc Inst Mech Eng H 220:345
41. Sommer S, Lauze F, Hauberg S, Nielsen M (2010) Manifold valued statistics, exact principal geodesic analysis and the effect of linear approximations. Eur Conf Comput Vis LNCS 6316:43–56
42. Zhang YZ, Lu S, Yang Y, Xu YQ, Li YB, Pei GX (2011) Design and primary application of computer-assisted, patient-specific navigational templates in metal-on-metal hip resurfacing arthroplasty. J Arthroplasty 26(7):1083–1087